Journal of Hazardous Materials 169 (2009) 233–239

Contents lists available at ScienceDirect

Journal of Hazardous Materials

journal homepage: www.elsevier.com/locate/jhazmat

Enhanced adsorptive and photocatalytic achievements in removal of methylene blue by incorporating tungstophosphoric acid–TiO_2 into MCM-41

M.A. Zanjanchi*, H. Golmojdeh, M. Arvand

Department of Chemistry, Faculty of Science, University of Guilan, P.O. Box 1914, Rasht, Iran

ARTICLE INFO

Article history:
Received 15 December 2008
Received in revised form 3 February 2009
Accepted 19 March 2009
Available online 27 March 2009

Keywords:
Photocatalysis
TiO_2
Tungstophosphoric acid
MCM-41
Methylene blue

ABSTRACT

The use of titania-dispersed materials in photocatalytic processes has been proposed as an alternative to the conventional bare TiO_2, in order to modify the surface area and activity of the catalyst. A homogeneously dispersed Keggin unit into TiO_2 was synthesized using tungstophosphoric acid (TPA) and titanium tetraisopropoxide. This compound was then loaded into MCM-41 by dispersing it in a suspension containing the mesoporous phase. Two other titanium-containing MCM-41 catalysts, Ti–MCM-41 and TiO_2/MCM-41 were also prepared using isomorphous substitution synthesis method and impregnation method, respectively, for the sake of comparison. The prepared photocatalysts were characterized by X-ray diffraction (XRD), nitrogen physisorption (BET) and chemical analysis. The catalysts were used to study degradation of methylene blue (MB) in aqueous solution. XRD result shows a pure anatase crystalline phase for TPA-containing TiO_2 indicating that there is good molecular distribution of tungstophosphoric acid into TiO_2 structure. Supported TPA–TiO_2 into MCM-41 shows both TPA–TiO_2 and MCM-41 characteristic X-ray reflections in the high-angle and low-angle parts of the XRD patterns, respectively. The experimental results show that adsorption is a major constituent in the elimination of MB from the dye solutions by the TPA-containing materials. Exploitation of both adsorption and photocatalytic processes speeds up the removal of the dye using the TPA–TiO_2-loaded MCM-41 photocatalyst. The elimination of MB is completed within 15 min for a 30 mg l^{-1} MB solution containing a catalyst dose of 100 mg/100 ml. The efficiencies of the other photocatalysts such as commercial TiO_2, Ti–MCM-41, TiO_2/MCM-41 and TPA–TiO_2 for adsorption and degradation of MB were also studied and compared with that of the prepared catalyst.

1. Introduction

In recent years, there has been a magnificent amount of research and development in the area of photocatalytic degradation and heterogeneous photocatalysis. Heterogeneous photocatalysis is an attractive and highly efficient method for degradation of toxic and non-biodegradable environmental pollutants commonly present in domestic or industrial wastewater [1–9]. These processes are based on the use of UV radiation to excite a semiconductor material, usually TiO_2, which on its surface the oxidation of the pollutants is performed. TiO_2 is chemically and biologically inert, photocatalytically stable, commercially available and inexpensive, and environmentally friendly [2,10]. However, there are certain limitations of using bare TiO_2 in photocatalyst reactors. To have an adequate TiO_2 photocatalytic activity, particles should be small enough to offer a high specific surface area. But due to this small size (about 30 nm) TiO_2 aggregates rapidly in a suspension loosing its effective surface area as well as the catalytic efficiency. In addition to that, application of such small particles imposes a high filtration costs to remove the catalyst when the reaction is finished. These problems have prompted the development of supported photocatalysts in those TiO_2 has been immobilized on the porous adsorbent materials. Some of the recent studies have reported the use of silica [11–13], clay [14], polymer film [15], activated carbon [16–18], and zeolites [19,20] as an effort to increase the efficiency and performance of the catalysts.

In the last decade, supporting TiO_2 on the mesoporous materials [19–26] has attracted considerable attention because of their very large surface area, controllable pore size and narrow pore size distribution. They are usually loaded with TiO_2 by sol–gel [21–24] or impregnation [19,20,25] methods. One of the most interesting mesoporous materials is MCM-41 which is an inorganic silica based material and exhibits a uniform hexagonal arrangement of cylindrical pores. Although, numerous works have been reported on the immobilization of TiO_2 on MCM-41 materials, detailed characterization and performance evaluation in different applications are lacking.

* Corresponding author. Tel.: +98 131 3226643; fax: +98 131 3220066.
E-mail addresses: zanjanchi@guilan.ac.ir, mazanjanchi@yahoo.com (M.A. Zanjanchi).

0304-3894/$ – see front matter © 2009 Elsevier B.V. All rights reserved.
doi:10.1016/j.jhazmat.2009.03.080

Another approach to increase surface area of TiO_2 and therefore to improve its catalytic activity is to make mesoporous TiO_2. This is achieved by using suitable pore-forming agents including surfactants [27,28] or organic compounds [29,30]. However, synthesizing mesoporous TiO_2 is not as simple as that of mesoporous silica due to higher reactivity of the former towards hydrolysis and condensation [31]. If this reactivity is not controlled, the synthesis will lead to an ill-defined and poorly ordered structure. Therefore, there are methods and challenges to synthesize stable mesoporous TiO_2 with a high surface area and suitable ordered form [32–35]. Recently, Huang et al. reported synthesis of mesoporous TiO_2 particles using tungstophosphoric acid at the absence of any template [36]. The material lacks long-range ordering of pores because of the absence of template that controls the packing of micellar rods. Yang et al. have also reported synthesis of TiO_2 photocatalyst containing homogeneously dispersed tungstophosphoric acid by combined sol–gel and programmed temperature hydrothermal method [37]. Their composite materials show photocatalytic activity for decomposition of various organic dyes. They suggested that the higher photocatalytic activity of tungstophosphoric acid–TiO_2 compared to traditional TiO_2 is mainly originated from the synergistic effect produced by the combination of polyoxotungstate unit ($H_3PW_{12}O_{40}$) and TiO_2. According to this consequence, the interfacial electron transfer takes place from the TiO_2 conduction to $H_3PW_{12}O_{40}$ after irradiation. Such an effective electron transfer can inhibit the fast electron–hole recombination on TiO_2.

In this contribution, we tried to improve the activity of $H_3PW_{12}O_{40}$–TiO_2 composite (TPA–TiO_2) by supporting it onto MCM-41 (a mesoporous material) to combine the synergestic effect of the former with the high stability and large surface area of the later. Modification of the surface of MCM-41 by introduction of bulky group of TPA–TiO_2 to its structure produced an efficient adsorbent and photocatalyst based on TiO_2. This catalyst is used for photodegradation and mineralization of methylene blue. Methylene blue is a pollutant dye chosen as the model compound to determine the photocatalytic activity of the supported TiO_2 in aqueous medium. The performance of the supported TiO_2 in degradation of the dye is studied under different operating conditions and the results are compared with that of commercially available TiO_2[−].

2. Experimental

2.1. Reagents and materials

The commercially available TiO_2 powder was in anatase crystalline form with purity of 99% purchased from Merck. Tetraethyl orthosilicate (TEOS) was purchased from ACROS. N-cetyl-N,N,N-trimethyl ammonium bromide (CTMABr), tungstophosphoric acid ($H_3PW_{12}O_{40}$: TPA), ethylamine, ethanol, methylene blue, HCl, isopropanol and tetraisopropyl orthotitanate (titanium tetraisopropoxide) were obtained from Merck.

2.2. Preparation of photocatalyst

The TPA–TiO_2 composite was prepared with little modification in the described procedure in the literature [37]. In a typical experiment, 6 ml titanium tetraisopropoxide (TTIP, 98%) was dissolved in 30 ml of isopropyl alcohol while stirring was used. In another container, 0.4 g of $H_3PW_{12}O_{40}$ (TPA) was dissolved in 0.8 ml of water and then it was added into the TTIP solution drop by drop. The resulting mixture was adjusted to pH 1–2 by the addition of 8 mol l^{-1} HCl, and then stirred at room temperature for 1 h. The mixture was heated to 45 °C until homogeneous hydrogel was formed. This hydrogel was transferred into an autoclave, and then heated to 200 °C at a heating rate of about 2 °C min^{-1}. Finally the temperature was kept at 200 °C for 1 h. After cooling the TPA–TiO_2 hydrogel to room temperature, it was dehydrated slowly at 50 °C for 24 h. The dried gel was washed with hot water three times, and then dried at room temperature. The product is white powder.

The parent purely siliceous MCM-41 was synthesized by a room-temperature synthesis method as described previously [38]. We used TEOS as a source of silicon and CTMABr as template for preparation of MCM-41. The procedure for MCM-41 synthesis is as follows: 2.7 g ethylamine was added to 42 ml of deionized water and the mixture was stirred at room temperature for 10 min. The amount, 1.47 g of surfactant (CTMABr) was gradually added to the above solution under stirring for 30 min. After further stirring 30 min, a clear solution was obtained. Then, 2.1 g TEOS solution was added drop wise to the solution. The molar composition of the mixture was:

$$SiO_2 : 1.6\ EA : 0.215\ CTMABr : 125H_2O$$

The pH of the reaction mixture was adjusted to 8.5 by the slow addition of hydrochloric acid solution (1 M) to the mixture. At this stage, the precipitate is formed. After 2 h, under slow stirring, the precipitate was separated and washed by centrifugation. The sample was dried at 45 °C for 12 h.

Titanium-containing MCM-41 samples with different 5, 50 and 100 Si/Ti molar ratios were also prepared by a direct isomorphous substitution synthesis method. The procedure is similar to the method described above for siliceous MCM-41 but with the addition of Ti source (titanium tetraisopropoxide) in appropriate amounts. The MCM-41 and Ti–MCM-41 samples were calcined at 550 °C for 5 h to decompose the surfactants and obtain the white powder. The Ti–MCM-41 with a high content of Ti (Si/Ti ratio of 5) was used for photocatalytic experiments.

TPA–TiO_2 incorporated MCM-41 was prepared based on some modification in the described procedure previously reported in the literature [39]. 0.05 g of our prepared TPA–TiO_2 was dispersed in distilled water and a few drops of diluted HCl was added to avoid possible hydrolysis of the compound. Then 0.05 g of the calcined MCM-41 was added to make a suspension. The suspension was stirred and evaporated at 80 °C until dryness. Then the solid was ground to fine particles and dried at 200 °C for 6 h in air flowing oven. The catalyst prepared by this method was named TT–MCM-41.

Also, 0.05 g of commercial TiO_2 and 0.05 g of MCM-41 were mixed using 2 ml ethanol in agate pestle and mortar. The solvent was then removed by evaporation while mixing. Samples prepared by this method were dried at 110 °C and calcined in air at 450 °C for 6 h. This sample is designated as TiO_2/MCM-41.

2.3. Characterization and measurement methods

A Philips PW1840 X-ray diffractometer with Cu Kα radiation was used to record the powder XRD patterns. The BET specific surface area of catalysts was determined by nitrogen adsorption at liquid nitrogen temperature on a Sibata SA-1100 surface area analyzer. Elemental chemical analysis of the catalysts was done by XRF method using a Bruker, S4 Pioneer model.

The photochemical reactor was a beaker containing suspension of methylene blue (MB) solution and solid photocatalyst which was placed in a continuously ventilated chamber. The suspension was magnetically stirred before and during irradiation. UV illumination was done with a 400 W Kr lamp (Osram). The illumination power of the lamp is mainly in the UV-A region. More precisely, ≈90% of the radiated power is in the UV-A region (400–315 nm) and about 10% in the UV-B region (315–280 nm). The distance between the lamp and the reactor was 30 cm for each experiment. Prior to irradiation, the sample was stirred for 5 min to establish an adsorption–desorption equilibrium between the catalyst surface and the dye. After

Table 1
Preparation method, surface area and pore volume for TiO_2, MCM-41 and the prepared TiO_2 catalysts.

Sample	Preparation method	Surface area (m^2/g)	Pore volume (cm^3/g)
TiO_2	Commercial titanium dioxide (Merck)	10.6	–
TPA–TiO_2	Sol–gel using tungstophosphoric acid and titanium tetraisopropoxide	110	–
MCM-41	Room-temperature synthesis	1090	0.39
TiO_2/MCM-41	Impregnation	590	0.21
Ti–MCM-41	Isomorphous substitution using titanium tetraisopropoxide	750	0.27
TT–MCM-41	Loading TPA–TiO_2 from suspension	450	0.16

irradiation, regular sampling and removal of the photocatalyst particles by centrifugation, the residual dye concentration was analyzed by spectrophotometric method. A double beam Shimadzu UV-2100 spectrophotometer was used for the determination of dye concentration. All the experiments were conducted at room temperature. The aqueous dye/catalyst suspension was prepared by the addition of 100 mg catalyst to a 100 ml aqueous solution of dye. Initial concentration of methylene blue was 30 mg l^{-1} in all of the experiments. A neutral media of pH 7 was used in all experiments. In some experiments H_2O_2 was added to reaction mixture to make a 0.05 M or other concentrations. For a dark adsorption experiment, 100 mg of adsorbent was added to 100 ml of 30 mg l^{-1} MB solution and the mixture was stirred for 60 min in the dark.

3. Results and discussion

3.1. Characterization

The designations for different prepared materials are summarized in Table 1. The preparation method, specific surface area and pore volume for the samples are shown in the table. The surface area and pore volume were calculated using data of the liquid nitrogen physisorption experiments. As it is evident from Table 1, by introduction of TPA units into TiO_2 structure via our sol–gel procedure using titanium tetraisopropoxide, the TPA–TiO_2 acquire a surface area much greater than our commercially obtained TiO_2. The table shows that our synthesized MCM-41 has a very large surface area (1090 m^2/g) and large pore volume (0.39 cm^3/g). However, after loading TiO_2 into MCM-41 structure, the surface area and the pore volume of TiO_2/MCM-41 sample are significantly reduced in comparison with those of pure MCM-41. Indeed, the surface area for TiO_2/MCM-41 is almost the average of the surface area of both components of the samples: TiO_2 and MCM-41 (Table 1). This result is expected because the surface area of TiO_2 is insignificant in comparison with that of MCM-41. The thermal treatment at 450 °C does not produce a further reduction of the surface area of the components, because MCM-41 was previously calcined at higher temperature (550 °C). The amount of surface area reduction is more for TT–MCM-41, in spite that the surface area of TPA–TiO_2 is 10 times higher than that of TiO_2 and that this sample was dried at a low temperature (200 °C). Accordingly, the pore volume is notably lower than in MCM-41. These results may indicate that TPA–TiO_2 units are incorporated inside the pores of the MCM-41 matrix. The changes in the XRD pattern at low angle (Fig. 2), with respect to pure MCM-41, also indicate a strong interaction between TPA–TiO_2 and MCM-41. The reduction in the surface area and pore volume for Ti–MCM-41 may really be related to the changes in the microstructure and some disordering in the structure which may happens during isomorphous-substitution process.

X-ray diffraction patterns of TiO_2 and TPA–TiO_2 samples are shown in Fig. 1. The characteristics diffraction peaks for anatase TiO_2 structure can be verified by inspection of XRD patterns [40]. The main XRD peak for anatase appears at $2\theta = 25.3^\circ$ with others indexed and shown in Fig. 1a. XRD patterns of TPA–TiO_2 shows the same feature as anatase without any indication of tungstophosphoric acid crystalline phase. Therefore, TPA units are successfully introduced into TiO_2 structure rather than existing in separate free solid phase. The molecular distribution of TPA units into TiO_2 and forming a stable composite could be occurred during the process of hydrolysis of titanium tetraisopropoxide in the presence of tungstophosphoric acid. In this process the Keggin units entrapped by the titania network, interact with internal surface hydroxyl group of titania producing the $(TiOH_2^+)(H_2PW_{12}O_{40}^-)$ composite [37]. However, due to this interaction and because of taking up the $H_3PW_{12}O_{40}$ units by TiO_2, some disorder in the TiO_2 structure happens and therefore, the crystallinity of our TPA–TiO_2 was poor compared to that of TiO_2.

Fig. 2 shows low angle XRD patterns of MCM-41, TiO_2/MCM-41, Ti–MCM-41 and TT–MCM-41 samples. The characteristic MCM-41 reflections related to the ordered hexagonal mesoporous structure are confirmed [41,42]. The recorded XRD pattern for Ti–MCM-41 is similar to MCM-41 but the intensity of the main diffraction peak for TiO_2/MCM-41 and TT–MCM-41 is reduced considerably. This is

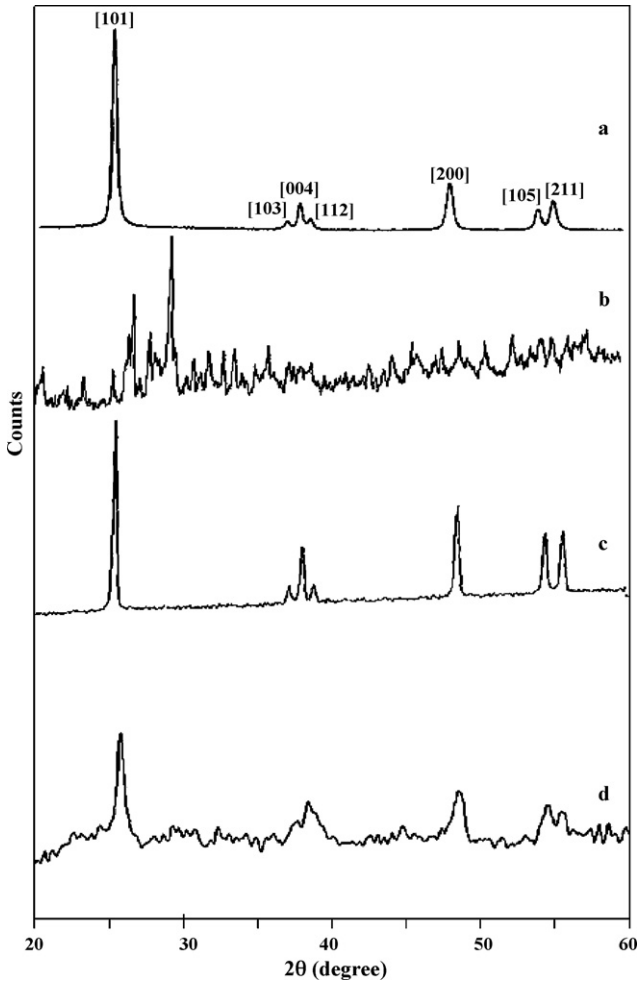

Fig. 1. X-ray diffraction patterns of (a) pure anatase, (b) tungstophosphoric acid (TPA), (c) TiO_2 and (d) TPA–TiO_2.

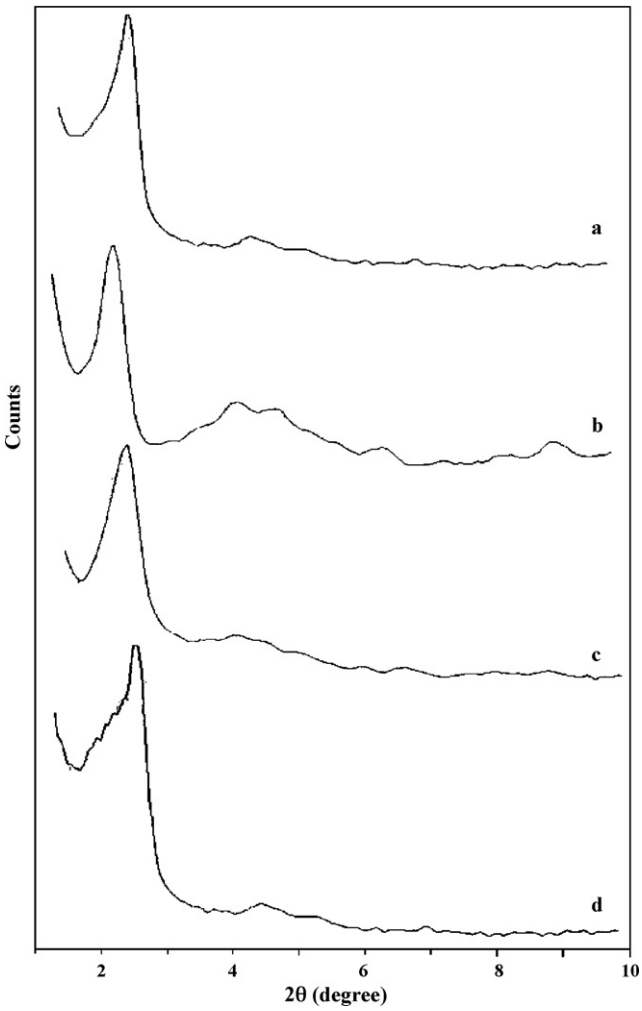

Fig. 2. X-ray diffraction patterns of (a) MCM-41, (b) TiO_2/MCM-41, (c) Ti–MCM-41 and (d) TT–MCM-41.

possibly arisen from the post-synthesis treatment carried out on these latter samples. For Ti–MCM-41 sample where Ti is introduced during the synthesis time a more ordered structure similar to MCM-41 was obtained.

The XRD pattern for Ti–MCM-41 within the range of $2\theta = 20–60^\circ$ (Fig. 3a) does not show the characteristic diffraction peaks of the anatase TiO_2 structure except a weak reflection at $2\theta = 25.3^\circ$. It should be mentioned that we did not observed this peak in the lower titanium-containing materials (i.e. Ti–MCM-41 with Si/Ti ratio of 50 and 100). Therefore, our photocatalyst Ti–MCM-41 sample with Si/Ti ratio of 5 contains low amount of free TiO_2 particles. Inspection of the XRD pattern for TT–MCM-41 within range $2\theta = 20–60^\circ$ shows the presence of characteristic anatase reflections quite similar to those observed for TPA–TiO_2 in Fig. 1d. This indicates that the TPA–TiO_2 units are incorporated into the structure of MCM-41 as the consequence of adding MCM-41 to a suspension containing our pre-prepared TPA–TiO_2. There is strong interaction between both compounds as it is indicated by the changes in the XRD pattern at low angles (Fig. 2), with respect to pure MCM-41.

To check the interaction of the loaded TPA–TiO_2 units to the MCM-41 support, a leaching test was performed on TT–MCM-41 sample. For this purpose, 0.1 g of TT–MCM-41 was stirred in 100 ml of deionized water for 24 h. Concentration of the tungstophosphoric acid leached into the water was determined by UV–vis spectrophotometric analysis. It was found that a negligible amount of 1.27% of TPA was leached out. This shows that TPA–TiO_2 units are retained

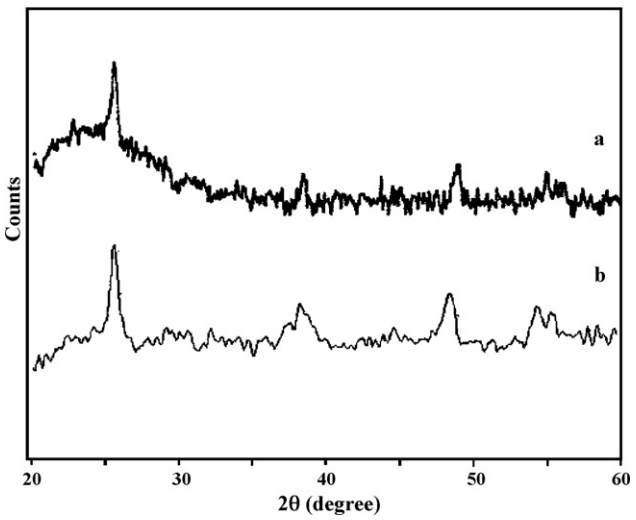

Fig. 3. X-ray diffraction patterns of (a) Ti–MCM-41 and (b) TT–MCM-41 at higher two theta angles.

in the MCM-41 because of relatively strong interaction of the units with MCM-41 host.

3.2. Adsorption studies

The dark adsorption study of methylene blue on supported catalysts and unsupported TiO_2 is presented in Table 2. There is a very sharp decrease of the concentration of MB within the first 5 min stirring in the dark upon the use of either TPA–TiO_2 or TT–MCM-41. The table shows that nearly all amount of the dye (in a 100 ml solution of MB with a concentration of 30 mg l^{-1} and 100 mg adsorbent) are adsorbed onto TT–MCM-41 or TPA–TiO_2 within 5 min. MCM-41 and titanium-incorporated MCM-41 samples (TiO_2/MCM-41 and Ti–MCM-41) show little adsorption of the dye following the first 5 min stirring in the dark, but adsorption of MB by the bare TiO_2 within the same time is approximately zero (Table 2). This indicates the importance of increased surface area in adsorption. It is interesting to note that although the surface area for TPA–TiO_2 is much lower than TT–MCM-41 (see Table 1), its adsorptive property is very close to that of TT–MCM-41 at our experimental condition. Extending the time of adsorption of the dye onto all the adsorbents (catalysts) for up to 60 min was resulted in rise of the adsorption of MB onto MCM-41-containing materials. About half of the initial amounts of the dye are adsorbed onto TiO_2/MCM-41 and Ti–MCM-41 and more than half of it is adsorbed onto MCM-41 following a 60 min adsorption in the dark.

In a series of separate experiments, adsorption of higher concentration of MB onto some of the samples was performed for a longer contact time (24 h) in the view of purposing them solely as adsorbents. For these samples, adsorption parameters were evaluated using the Langmuir adsorption isotherm, which is given by

Table 2
Adsorptive ability of the catalysts for methylene blue.

Sample	Initial concentration (mg l^{-1})	Conc. after 5 min (mg l^{-1})	Conc. after 60 min (mg l^{-1})
TiO_2	30	30	29
TPA–TiO_2	30	5	4
MCM-41	30	22	12
TiO_2/MCM-41	30	24	17
Ti–MCM-41	30	23	14
TT–MCM-41	30	3	0

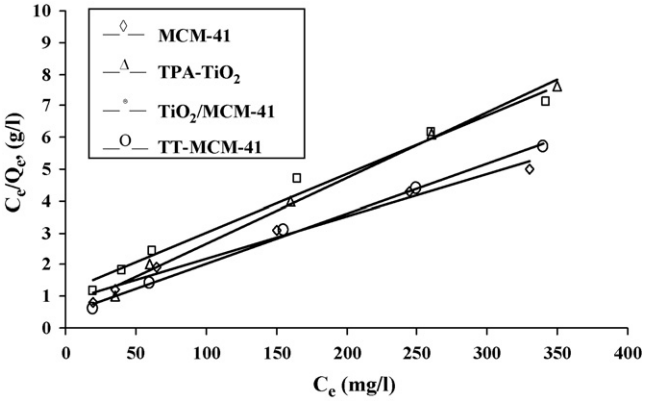

Fig. 4. Langmuir adsorption of methylene blue on various adsorbents. 100 mg of the adsorbent was stirred in 100 ml of the dye solution with an initial concentration range 30–400 mg l^{-1} for 24 h.

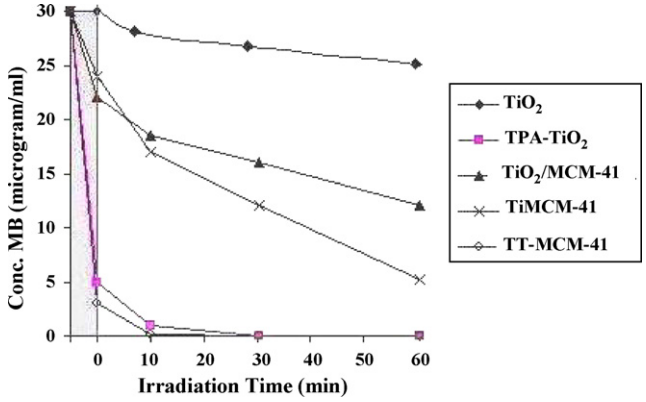

Fig. 5. Concentration changes of methylene blue as a function of irradiation time. The shaded area shows decrease of concentration of methylene blue due to adsorption at the first 5 min stirring in the dark. The concentration of MB was 30 mg l^{-1}, the weight of catalyst was 100 mg, volume of the dye solution 100 ml, concentration of H_2O_2 was 0.05 mol l^{-1}, photocatalytic reaction under 400 W UV irradiation at room temperature and the system was open to air.

equation below:

$$\frac{C_e}{Q_e} = \frac{1}{Q_{max}K_L} + \frac{C_e}{Q_{max}}$$

In this equation Q_e is the equilibrium MB concentration on adsorbent (mg/g), C_e is the equilibrium MB concentration in solution (mg l^{-1}), Q_{max} is the monolayer capacity of adsorbent (mg/g), and K_L is the Langmuir adsorption constant (l mg^{-1}). A plot of C_e/Q_e vs. C_e will give a straight line with slope $1/Q_{max}$ and intercept $1/(Q_{max}K_L)$. Fig. 4 shows the adsorption isotherms and Table 3 shows the calculated Langmuir adsorption parameters for the selected samples. Higher Q_{max} for MCM-41 in comparison with that of TT–MCM-41 (Table 3) and comparing these data with the related ones in Table 2 shows higher adsorption of MB by MCM-41 within a longer time of 24 h. Table 3 shows that K_L, Langmuir adsorption constant, is very similar for TPA–TiO_2 and TT–MCM-41and also both constants are larger than the others.

3.3. Photocatalytic degradation of methylene blue

Initially, control tests on degradation of MB were carried out in specified conditions described below. In a test, 100 ml solution of MB (30 mg l^{-1}) containing H_2O_2 (0.05 mol l^{-1}) placed in darkness. There was no noticeable decrease in MB concentration after 60 min. In a separate test, the same solution (in absence of H_2O_2) was exposed to UV irradiation for 60 min. Again, no considerable decrease in concentration of MB was observed. These results show that presence of H_2O_2 or UV irradiation alone cannot destruct the dye. However, exposing the MB solution containing hydrogen peroxide to UV irradiation will be effective in the degradation of MB. The amount of destructed MB, yet, is not considerable. In presence of 0.05 mol l^{-1} of hydrogen peroxide, only 3% of the dye is destructed following a 60 min irradiation run. This is expected because combination of UV-A irradiation + H_2O_2 does not lead to appreciable degradation of MB (90% of the intensity of the UV lamp is within the range of 400–315 nm). Increasing the concentration of hydrogen peroxide to 0.5 mol l^{-1} will raise amount of the dye degradation to about 15% under the same illumination type and within the same irradiation time. Addition of more hydrogen peroxide does not change the quantity of degradation of MB to a higher value.

Table 3
Adsorption parameters for selected catalysts.

Sample	K_L (l mg^{-1})	Q_{max} (mg/g)	r_L^2
MCM-41	0.0174	73.5	0.982
TiO_2/MCM-41	0.0161	54.3	0.980
TPA–TiO_2	0.0346	49.7	0.996
TT–MCM-41	0.0368	61.7	0.991

Photocatalytic ability of our prepared catalysts in adsorbing and degradation of MB has been shown in Fig. 5. The data are obtained following a two step experiments. At first period the mixture of the catalyst and dye solution was stirred for 5 min in the dark and then the mixture was exposed to UV light and was irradiated for 60 min. Fig. 5 clearly shows a sharp decrease in concentration of MB in the initial 5 min for TPA–TiO_2 and TT–MCM-41 which is due to adsorption. Then the reduction of the dye concentration is continued with a gentle slope which is due to photodegradation. This indicates that the higher surface area and adsorption capacity for TPA–TiO_2 and TT–MCM-41 compared to that of bare TiO_2 plays the major role for elimination of MB. Obviously, achieving greater adsorption for MB is mainly related to the presence of tungstophosphoric acid in both TPA–TiO_2 and TT–MCM-41. Fig. 5 clearly shows that none of the TiO_2/MCM-41 and Ti–MCM-41 samples can adsorb that amount of MB within the first 5 min step (dark adsorption) even though they contain MCM-41. TiO_2/MCM-41 and Ti–MCM-41 have surface area much higher than TPA–TiO_2 and higher than TT–MCM-41 (see Table 1). An explanation for the rise of adsorption capacity for these tungstophosphoric acid-containing materials may be proposed. It is generally believed that emerging of negative charges in the structure of solids improves adsorption of a cationic species. This may be related to the change of zeta potential in our tungstophosphoric acid-containing composite materials. The point of zero charge of the TiO_2 (Degussa P25) is at pH 6.8 [43]. This means the TiO_2 surface is positively charged at pH < 6.8, whereas, it is negatively charged at pH > 6.8. However, this point of zero charge may be changed to the lower values in the supported catalysts [24]. The change of the isoelectric point to lower values, in parallel with the amount of tungstophosphoric acid species incorporated into mesoporous titanium oxide, has been well established now [44]. Fuchs et al. have found that the pH of the isoelectric point of titanium oxide which is regarded as 6.5 for a pure mesoporous anatase, will decrease to the pH values 6.2, 6.0 and 5.5 for the TiO_2 samples containing 10, 20 and 30% TPA, respectively [44]. Therefore, the following surface reaction for the supported catalysts is expected to occur at our experimental condition:

$$TiOH + OH^- \rightarrow TiO^- + H_2O$$

The electrical charge of the solid surface of TPA–TiO_2 and TT–MCM-41 would strongly affects adsorption of cationic MB^+ dye molecules.

Table 4
Adsorption and photocatalytic ability of prepared catalysts, bare TiO_2 and MCM-41 for the removal of methylene blue[a].

Catalyst	Conversion (%)[b] (5 min)	Conversion (%)[b] (15 min)
TiO_2	0.7	3.0
MCM-41	9.0	44
TiO_2/MCM-41	20	43
Ti–MCM-41	24	47
TPA–TiO_2	83	93
TT–MCM-41	90	100

[a] The concentration of MB was 30 mg l^{-1}, the weight of catalyst was 100 mg, volume of the dye solution 100 ml, concentration of H_2O_2 was 0.05 mol l^{-1}, photocatalytic reaction under 400 W UV irradiation at room temperature and the system was open to air.

[b] Conversion (%) is defined as $(C_0 - C_t)/C_0 \times 100$, C_0 and C_t are concentration of MB at time 0 and t. Samples were stirred for 5 min in darkness and then exposed to UV irradiation.

The rate of elimination of the dye molecules contained in 100 ml solution of MB with an initial concentration 30 mg l^{-1} and at presence of 100 mg TT–MCM-41, is so high that all of the dye is removed within 15 min. Fig. 5 shows a sharp lowering of the concentration to 10% of its initial value following the first 5 min stirring in the dark. At this stage, elimination of the dye molecules is due to adsorption. Degradation of MB will be started upon exposing the solution to the UV light. Table 4 compares the conversion percent of MB after 5 and 15 min time from the beginning (5 min in the dark and 10 min under UV irradiation). Complete removal of MB is achievable in 15 min using TT–MCM-41 catalyst (Table 4).

From the standpoint of separation and recovery of the catalyst and evaluating the ability of the used catalyst for elimination of the dye, two methods were employed. The high-temperature calcination and hot ethanol-washing followed by ultrasonic-bath were performed for regeneration of the used TT–MCM-41. In the high-temperature calcinations process the used TT–MCM-41 was placed in a furnace with static air and calcined it with a heating rate of 5° C min^{-1} from room temperature to 450 °C. In the second method, the used materials were washed with hot ethanol and placed in an ultrasonic-bath for 10 min. Most of the dye species are removed from the catalyst (adsorbent), however, the recovered catalysts showed gradual decreasing of the adsorption capacity and consequently lower efficiency. The decreasing of the efficiency is more severe for the heated samples. The ability of TT–MCM-41 for removing the dye reduces to 20% of the fresh catalyst following three successive use of the catalyst exploiting the hot ethanol-washing method. It seems that both of the high-temperature calcination method and hot ethanol-washing followed by ultrasonic-bath treatment may deteriorate the interaction between TiO_2–TPA units and MCM-41. Calcination at high-temperature may even affect the stability of TPA molecules incorporated into TiO_2 matrix [45]. Further work is needed for complete elucidating of this matter.

Although, TT–MCM-41 is surely the best material for elimination of MB, it is not the most active photocatalyst among our samples. The photocatalytic activity could be estimated by considering the rate of the dye disappearance just after turning the UV source on (after the initial 5 min). The catalyst activity sequence for MB elimination was found as below:

$$\text{Ti–MCM-41}(0.71) > \text{TPA–TiO}_2(0.34)$$
$$\approx \textit{TiO}_2/\text{MCM-41}(0.33) \approx \text{TT–MCM-41}(0.31) > \text{TiO}_2(0.22)$$

The numbers in parentheses correspond to the slope of the degradation curves shown in Fig. 5 after the initial 5 min stirring in the dark. It is obvious that Ti–MCM-41 is the most active photocatalyst. The photocatalytic activities of TT–MCM-41, TPA–TiO_2 and TiO_2/MCM-41 are approximately the same. The commercial TiO_2 showed the lowest catalytic activity. We believe that proper distribution of titanium oxide into MCM-41 structure which can be originated via isomorphous substitution method imparts the highest catalytic activity to Ti–MCM-41. However, this sample is not a strong adsorbent due to lack of TPA in its composition. As mentioned above, the presence of TPA in TPA–TiO_2 and in TT–MCM-41 and shifting the pH of the point of zero charge to lower values for these materials, generate strong adsorption sites at our experimental condition.

4. Conclusion

The photocatalytic degradation of methylene blue over several types of TiO_2-containing materials was investigated. The examined photocatalysts include TiO_2/MCM-41 prepared by impregnation method, Ti–MCM-41 prepared by isomorphous substitution, TPA–TiO_2 by dispersion of tungstophosphoric acid into TiO_2 structure and TPA–TiO_2 composite loaded onto MCM-41 (TT–MCM-41) by suspension procedure. Our results show that TT–MCM-41 is the most efficient material among them and effectively removes methylene blue from solution in a very short time. Elimination is completed within 15 min for a 30 mg l^{-1} methylene blue solution containing a catalyst dose of 100 mg/100 ml. Adsorption has a significant role for the very high efficiency of this photocatalyst for elimination of methylene blue. Although the surface area is higher for TiO_2/MCM-41 and Ti–MCM-41, but presence of tungstophosphoric acid–TiO_2 composite in the MCM-41 structure makes TT–MCM-41 the most active material for complete removal of methylene blue within a short time. The strong adsorptive capacity of TT–MCM-41 can be combined with its photocatalytic activity in achieving a rapid removal of the dye.

Acknowledgement

The authors wish to acknowledge the financial support of the Research Department of the University of Guilan.

References

[1] M.R. Hoffmann, S.T. Martin, W. Choi, D.W. Bahnemann, Environmental applications of semiconductor photocatalysis, Chem. Rev. 95 (1995) 69–96.
[2] A.L. Linsebiger, G. Lu, J.T. Yates, Photocatalysis on TiO_2 surfaces: principles, mechanisms, and selected results, Chem. Rev. 95 (1995) 735–758.
[3] J.M. Herrmann, Heterogeneous photocatalysis: fundamentals and applications to the removal of various types of aqueous pollutants, Catal. Today 53 (1999) 115–129.
[4] A. Fujishima, T.N. Rao, D.A. Tryk, Titanium dioxide photocatalysis, J. Photochem. Photobiol. C 1 (2000) 1–21.
[5] J.G. Yu, J.C. Yu, M.K.-P. Leung, W.K. Ho, B. Cheng, X.-J. Zhao, J.C. Zhao, Effects of acidic and basic hydrolysis catalysts on the photocatalytic activity and microstructures of bimodal mesoporous titania, J. Catal. 217 (2003) 69–78.
[6] M. Anpo, M. Takeuchi, The design and development of highly reactive titanium oxide photocatalysts operating under visible light irradiation, J. Catal. 216 (2003) 505–516.
[7] A. Fujishima, X. Zhang, Titanium dioxide photocatalysis: present situation and future approaches, Comptes Rendus Chimie 9 (2006) 750–760.
[8] S. Devipriya, S. Yesodharan, Photocatalytic degradation of pesticide contaminants in water, Sol. Energy Mater. Sol. Cells 86 (2005) 309–348.
[9] N.A. Garcia, F. Amat-Guerri, Photodegradation of hydroxylated *N*-heteroaromatic derivatives in natural-like aquatic environments: a review of kinetic data of pesticide model compounds, Chemosphere 59 (2005) 1067–1082.
[10] U. Diebold, The surface science of titanium dioxide, Surf. Sci. Rep. 48 (2003) 53–229.
[11] Y. Xu, W. Zheng, W. Liu, Enhanced photocatalytic activity of supported TiO_2: dispersing effect of SiO_2, J. Photochem. Photobiol. A: Chem. 122 (1999) 57–60.
[12] A. Amlouk, L. El Mir, S. Kraiem, S. Alaya, Elaboration and characterization of TiO_2 nanoparticles incorporated in SiO_2 host matrix, J. Phys. Chem. Solids 67 (2006) 1464–1468.
[13] J. Aguado, R. van Grieken, M.-J. López-Munoz, J. Marugán, A comprehensive study of the synthesis, characterization and activity of TiO_2 and mixed TiO_2/SiO_2 photocatalysts, Appl. Catal. A 312 (2006) 202–212.
[14] K. Shimizu, T. Kaneko, T. Fujishima, T. Kodama, H. Yoshida, Y. Kitayama, Selective oxidation of liquid hydrocarbons over photoirradiated TiO_2 pillared clays, Appl. Catal. A: Gen. 225 (2002) 185–191.

[15] M.R. Dhananjeyan, J. Kiwi, K.R. Thampi, Photocatalytic performance of TiO_2 and Fe_2O_3 immobilized on derivatized polymer films for mineralisation of pollutants, Chem. Commun. (2000) 1443–1444.
[16] J. Hermann, J. Matos, J. Ddisdier, C. Guillard, J. Laine, S. Malato, J. Blanco, Solar photocatalytic degradation of 4-chlorophenol using the synergistic effect between titania and activated carbon in aqueous suspension, Catal. Today 54 (1999) 255–265.
[17] H. Yoneyama, T. Torimoto, Titanium dioxide/adsorbent hybrid photocatalysts for photodestruction of organic substances of dilute concentrations, Catal. Today 58 (2000) 133–140.
[18] E.A. El-Sharkawy, A.Y. Soliman, K.M. Al-Amer, Comparative study for the removal of methylene blue via adsorption and photocatalytic degradation, J. Colloid Interf. Sci. 310 (2007) 498–508.
[19] Y.-H. Hsien, C.-F. Chang, Y.-H. Chen, S. Cheng, Photodegradation of aromatic pollutants in water over TiO_2 supported on molecular sieves, Appl. Catal. B: Environ. 31 (2001) 241–249.
[20] A. Bhattacharyya, S. Kawi, M.B. Ray, Photocatalytic degradation of orange II by TiO_2 catalysts supported on adsorbents, Catal. Today 98 (2004) 431–439.
[21] L. Davydov, E.P. Reddy, P. France, P.G. Smirniotis, Transition-metal-substituted titania-loaded MCM-41 as photocatalysts for the degradation of aqueous organics in visible light, J. Catal. 203 (2001) 157–167.
[22] B. Sun, E.P. Reddy, P.G. Smirniotis, TiO_2-loaded Cr-modified molecular sieves for 4-chlorophenol photodegradation under visible light, J. Catal. 237 (2006) 314–321.
[23] Y.-J. Do, J.-H. Kim, J.-H. Park, S.-S. Park, S.-S. Hong, C.-S. Suh, G.-D. Lee, Photocatalytic decomposition of 4-nitrophenol on Ti-containing MCM-41, Catal. Today 101 (2005) 299–305.
[24] G. Li, X.S. Zhao, M.B. Ray, Advanced oxidation of orange II using TiO_2 supported on porous adsorbents: the role of pH, H_2O_2 and O_3, Sep. Purif. Technol. 55 (2007) 91–97.
[25] N.B. Lihitkar, M.K. Abyaneh, V. Samuel, R. Pasricha, S.W. Gosavi, S.K. Kulkarni, Titania nanoparticles synthesis in mesoporous molecular sieve MCM-41, J. Colloid Interf. Sci. 314 (2007) 310–316.
[26] S. Anandan, Photocatalytic effects of titania supported nanoporous MCM-41 on degradation of methyl orange in the presence of electron acceptors, Dyes Pigments 76 (2007) 535–541.
[27] G.J.A.A. Soler-Illia, A. Louis, C. Sanchez, Synthesis and characterization of mesostructured titania-based materials through evaporation-induced self-assembly, Chem. Mater. 14 (2002) 750–759.
[28] V.F. Stone Jr., R.J. Davis, Synthesis, characterization, and photocatalytic activity of titania and niobia mesoporous molecular sieves, Chem. Mater. 10 (1998) 1468–1474.
[29] C. Wang, Q. Li, R.D. Wang, Synthesis and characterization of mesoporous TiO_2 with anatase wall, Mater. Lett. 58 (2004) 1424–1426.
[30] J.Y. Zheng, J.B. Pang, K.Y. Qui, Y. Wei, Synthesis of mesoporous titanium dioxide materials by using a mixture of organic compounds as a non-surfactant template, J. Mater. Chem. 11 (2001) 3367–3372.
[31] E. Beyers, P. Cool, E.F. Vansant, Stabilisation of mesoporous TiO_2 by different bases influencing the photocatalytic activity, Micropor. Mesopor. Mater. 99 (2007) 112–117.
[32] T. Peng, D. Zhao, H. Song, C. Yan, Preparation of lanthana-doped titania nanoparticles with anatase mesoporous walls and high photocatalytic activity, J. Mol. Catal. A 238 (2005) 119–126.
[33] T.Y. Peng, D. Zhao, K. Dai, W. Shi, K. Hirao, Synthesis of titanium dioxide nanoparticles with mesoporous anatase wall and high photocatalytic activity, J. Phys. Chem. B 109 (2005) 4947–4952.
[34] E. Beyers, P. Cool, E.F. Vansant, Anatase formation during the synthesis of mesoporous titania and its photocatalytic effect, J. Phys. Chem. B 109 (2005) 10081–10086.
[35] M.M. Mohamed, W.A. Bayoumy, M. Khairy, M.A. Mousa, Synthesis of micro–mesoporous TiO_2 materials assembled via cationic surfactants: morphology, thermal stability and surface acidity characteristics, Micropor. Mesopor. Mater. 103 (2007) 174–183.
[36] D. Huang, Y.J. Wang, L.M. Yang, G.S. Luo, Direct synthesis of mesoporous TiO_2 modified with phosphotungstic acid under template-free condition, Micropor. Mesopor. Mater. 96 (2006) 301–306.
[37] Y. Yang, Q. Wu, Y. Guo, C. Hu, E. Wang, Efficient degradation of dye pollutants on nanoporous polyoxotungstate–anatase composite under visible-light irradiation, J. Mol. Catal. A 225 (2005) 203–212.
[38] M.A. Zanjanchi, Sh. Asgari, Incorporation of aluminum into the framework of mesoporous MCM-41: the contribution of diffuse reflectance spectroscopy, Solid State Ionics 171 (2004) 277–282.
[39] M.I. Ahmad, S.M.J. Zaidi, S. Ahmed, Proton conducting composites of heteropolyacids loaded onto MCM-41, J. Power Sources 157 (2006) 35–44.
[40] J. Liqianga, S. b, C. Xiaojuna, X. Weimina, D. Zilic, F. Yaoguoc, Honggangb, The preparation and characterization of nanoparticle TiO_2/Ti films and their photocatalytic activity, J. Phys. Chem. Solids 64 (2003) 615–623.
[41] J.S. Beck, J.C. Vartuli, W.J. Ruth, M.E. Leonowiez, C.T. Kresge, K.D. Schmitt, C.T.-W. Chu, D.H. Olson, E.V. Sheppard, S.B. Higgins, J.B. Higgins, J.L. Schlenker, A new family of mesoporous molecular sieves prepared with liquid crystal templates, J. Am. Chem. Soc. 114 (1992) 10834–10843.
[42] Z. Luan, C. Cheng, W. Zhou, J. Klinowski, Mesopore molecular sieve MCM-41 containing framework aluminum, J. Phys. Chem. 99 (1995) 1018–1024.
[43] I. Poulios, I. Tsachpinis, Photodegradation of the textile dye Reactive Black 5 in the presence of semiconducting oxides, J. Chem. Technol. Biotechnol. 74 (1999) 349–357.
[44] V.M. Fuchs, E.L. Soto, M.N. Blanco, L.R. Pizzio, Direct modification with tungstophosphoric acid of mesoporous titania synthesized by urea-templated sol–gel reactions, J. Colloids Interf. Sci. 327 (2008) 403–411.
[45] P.A. Jalil, N. Tabet, M. Faiz, N.M. Hamdan, Z. Hussain, Surface investigation on thermal stability of tungstophosphoric acid supported on MCM-41 using synchrotron radiation, Appl. Catal. A 257 (2004) 1–6.